Journal of Visualized Experiments

Quantification of Mouse Heart Left Ventricular Function, Myocardial Strain, and Hemodynamic Forces by Cardiovascular Magnetic Resonance Imaging

--Manuscript Draft--

Article Type:	Invited Methods Collection - JoVE Produced Video
Manuscript Number:	JoVE62595R1
Full Title:	Quantification of Mouse Heart Left Ventricular Function, Myocardial Strain, and Hemodynamic Forces by Cardiovascular Magnetic Resonance Imaging
Corresponding Author:	Mariah Daal Amsterdam UMC - Locatie AMC: Amsterdam UMC Locatie AMC Amsterdam, NETHERLANDS
Corresponding Author's Institution:	Amsterdam UMC - Locatie AMC: Amsterdam UMC Locatie AMC
Corresponding Author E-Mail:	m.r.daal@amsterdamumc.nl
Order of Authors:	Mariah Daal
	Gustav Strijkers
	Claudia Calcagno
	Ruslan Garipov
	Rob Wüst
	David Hautemann
	Bram Coolen
Additional Information:	
Question	**Response**
Please specify the section of the submitted manuscript.	Bioengineering
Please indicate whether this article will be Standard Access or Open Access.	Open Access ($3900)
Please indicate the **city, state/province, and country** where this article will be **filmed**. Please do not use abbreviations.	Amsterdam, North-Holland, The Netherlands
Please confirm that you have read and agree to the terms and conditions of the author license agreement that applies below:	I agree to the Author License Agreement
Please provide any comments to the journal here.	

TITLE:

Quantification of Mouse Heart Left Ventricular Function, Myocardial Strain, and Hemodynamic Forces by Cardiovascular Magnetic Resonance Imaging

AUTHORS AND AFFILIATIONS:

Mariah R. R. Daal[1], Gustav J. Strijkers[1,2], Claudia Calcagno[2], Ruslan R. Garipov[3], Rob C.I. Wüst[1,4], David Hautemann[5], Bram F. Coolen[1]

[1]Department of Biomedical Engineering & Physics, Amsterdam University Medical Centers, Amsterdam Cardiovascular Sciences, University of Amsterdam, Amsterdam, The Netherlands
[2]BioMedical Engineering and Imaging Institute, Icahn School of Medicine at Mount Sinai, New York, NY, USA
[3]MR Solutions Ltd., Guildford, United Kingdom
[4]Laboratory for Myology, Department of Human Movement Sciences, Faculty of Behavioral and Movement Sciences, Vrije Universiteit Amsterdam, Amsterdam Movement Sciences, The Netherlands
[5]Medis medical imaging systems B.V., Leiden, The Netherlands

Email addresses of co-authors:

Gustav J. Strijkers	(g.j.strijkers@amsterdamumc.nl)
Claudia Calcagno	(claudia.calcagno@mssm.edu)
Ruslan R. Garipov	(ruslan.garipov@mrsolutions.com)
Rob C.I. Wüst	(r.wust@vu.nl)
David Hautemann	(dhautemann@medisimaging.com)
Bram F. Coolen	(b.f.coolen@amsterdamumc.nl)

Corresponding author:

Mariah R. R. Daal	(m.r.daal@amsterdamumc.nl)

SUMMARY:

This study describes a comprehensive cardiovascular magnetic resonance imaging (CMR) protocol to quantify the left ventricular functional parameters of the mouse heart. The protocol describes the acquisition, post-processing, and analysis of the CMR images as well as assessment of different cardiac functional parameters.

ABSTRACT:

Mouse models have contributed significantly to understanding genetic and physiological factors involved in healthy cardiac function, how perturbations result in pathology, and how myocardial diseases may be treated. Cardiovascular magnetic resonance imaging (CMR) has become an indispensable tool for a comprehensive *in vivo* assessment of cardiac anatomy and function. This protocol shows detailed measurements of mouse heart left ventricular function, myocardial strain, and hemodynamic forces using 7-Tesla CMR. First, animal preparation and positioning in the scanner are demonstrated. Survey scans are performed for planning imaging slices in various short- and long-axis views. A series of prospective ECG-triggered short-axis (SA) movies (or CINE images) are acquired covering the heart from apex to base, capturing end-systolic and end-diastolic phases. Subsequently, single-slice, retrospectively gated CINE images are acquired in a midventricular short axis, and in 2-, 3-, and 4-chamber views, to be reconstructed into high-temporal resolution CINE images using custom-built and open-source software. CINE images are subsequently analyzed using dedicated CMR image analysis software.

Delineating endomyocardial and epicardial borders in SA, end-systolic and end-diastolic CINE images allows for the calculation of end-systolic and end-diastolic volumes, ejection fraction, and cardiac output. The midventricular SA CINE images are delineated for all cardiac time frames to extract a detailed volume-time curve. Its time derivative allows for the calculation of the diastolic function as the ratio of the early filling and atrial contraction waves. Finally, left ventricular endocardial walls in the 2-, 3-, and 4-chamber views are delineated using feature-tracking, from which longitudinal myocardial strain parameters and left ventricular hemodynamic forces are calculated. In conclusion, this protocol provides detailed *in vivo* quantification of the mouse cardiac parameters, which can be used to study temporal alterations in cardiac function in various mouse models of heart disease.

INTRODUCTION:

Cardiovascular magnetic resonance (CMR) in small animals provides an accurate *in vivo* measurement of myocardial function, making CMR an optimal tool for preclinical research in cardiovascular disease. Due to the high spatial resolution and high contrast between blood and myocardium in CMR images, it is possible to delineate the endo- and epicardial contours and calculate myocardial mass and ventricular volumes[1,2]. Despite the high heart rates of up to 600 beats/min, the use of electrocardiogram (ECG) and respiratory triggering allows high-quality measurements of different cardiac phases (also called CINE images) without respiratory motion artifacts. In this way, multiple slices can be used to cover the heart from apex to base to extract systolic function parameters such as ejection fraction (EF), end-systolic volume (ESV), end-diastolic volume (EDV), and cardiac output (CO)[3]. Aside from basic systolic function assessment, additional CMR techniques have been recently developed to assess diastolic dysfunction[4], myocardial strain[5], and hemodynamic forces (HDF)[6].

ECG gating allows synchronization to the cardiac cycle by starting MR signal acquisition after detection of the R-peak and recording a defined number of cardiac phases during the R-R interval. However, the number of cardiac phases (frame rate) that can be acquired this way depends on the lowest possible repetition time (TR) the system can reach while maintaining an acceptable signal-to-noise ratio (SNR) and spatial resolution[4]. Furthermore, because the use of high magnetic field gradients can temporarily distort the ECG signal, the acquisition is usually stopped before the end-diastolic phase. Both factors limit the use of such scans to systolic function assessments, as the calculation of other cardiac functional parameters requires a better definition of the left ventricular (LV) volume-time curve.

High-frame-rate CINE images can be acquired by retrospective gating, whereby MR signal is continuously acquired during scanning, and an incorporated navigator echo after radiofrequency (RF) excitation detects cardiac and respiratory motion. Because the CMR acquisition is performed asynchronously with the cardiac motion, the acquired MR signals can then be assigned to a retrospectively chosen number of cardiac frames. In this way, if sufficient data is collected, high-frame-rate CINE images can be reconstructed[4,7]. This then allows for diastolic function assessment, represented by the ratio between the peak early filling rate (E') and peak late filling rate from atrial contraction (A').

In clinical research, CINE images can be analyzed with CMR feature-tracking to assess the myocardial strain and HDF[6,8]. Myocardial strain is a cardiac deformation parameter that measures the difference in percentages between the initial length (usually in end-diastolic length) and maximum length (usually in end-systole) of a myocardial segment[9]. Myocardial strain measurements can be of incremental value for assessing the LV function as strain values quantify myocardial wall shortening and thickening. A reduction in shortening function might be an indication of subendocardial fiber damage[10]. Alterations in myocardial strain can occur independent of EF and could be a precursor for underlying complications.

Specifically, the global longitudinal strain (GLS) and global circumferential strain (GCS) have been shown to be of added value in characterizing heart disease[10–12]. Similarly, HDF has been suggested to be a potential novel parameter to indicate altered cardiac function[6,13]. These HDF or interventricular pressure gradients (IVPG) drive the blood motion during ejection and filling of the heart and are affected by the momentum exchange between blood and myocardium, including the aortic and mitral valve[14,15].

In this study, a comprehensive protocol is described for performing robust small animal CMR measurements to quantify LV function, myocardial strain, and HDF of mouse hearts. It contains the necessary steps for animal preparation, data acquisition using both prospectively and retrospectively gated CINE images of the heart, as well as analysis with dedicated software capable of calculating the volumetric measurements, E'/A' ratio, myocardial strain, and HDF of the heart. This protocol can be used for the extensive assessment of LV function in various mouse models of cardiovascular disease.

PROTOCOL:

The described animal experiments are conducted in accordance with European Union guidelines for the welfare of laboratory animals (Directive 2010/63/EU) and were approved by the Academic Medical Center Animal Ethics Committee.

1. Setup and animal preparation

1.1. Prior to starting the experiment, make sure there is sufficient isoflurane anesthesia for at least 2 h, and that the battery available for ECG and respiratory monitoring is sufficiently charged. Make sure the scanner area is equipped with a working fume extraction tube to remove excess isoflurane.

1.2. Prepare the mouse cradle (**Figure 1A**), and turn on the animal heating system with the temperature set to 40 °C. Prepare the ECG/respiratory interface module and battery setup (**Figure 1B**), and start the software for real-time monitoring of ECG and respiratory signals (**Figure 1C**).

1.3. Remove the mouse from its housing cage and measure body weight.

1.4. Place the mouse in an anesthesia induction chamber under a fume hood extraction arm, and provide 3–4% isoflurane in a mixture of 0.2 L/min O_2 and 0.2 L/min medical air. After the animal is fully anesthetized, apply a small drop of eye ointment to each eye, and close the eyelids of the mouse.

1.5. Place the mouse in the supine position on the mouse cradle. Hook the incisors of the mouse in the bite bar on the mouse cradle, and adjust the nose cone to fit properly (**Figure 1A**). Visually check if the breathing is stable below 100 breaths/min, and reduce the isoflurane to ~2% during animal preparation.

1.6. Move the mouse cradle such that the heart is located in the part of the cradle holder that will end up in the center of the RF coil and iso-center of the magnet.

1.7. Use petroleum jelly to insert the rectal temperature probe, and tape the fiber-optic cable of the temperature probe to the mouse cradle.

1.8. Place the respiratory balloon on the lower abdomen of the mouse and secure it with tape. Insert two ECG electrode needles subcutaneously in the thorax at the height of the forepaws and gently tape them down to prevent movement (**Figure 1A**).

1.9. Check whether respiration and ECG signals are of sufficient quality, and whether correct trigger points are detected by the software (**Figure 1C**).

1.9.1. Make sure the respiratory rate is 50–80 breaths/min, heart rate ~400–600 beats/min, and body temperature around 37 °C. Adjust the isoflurane administration when the respiratory rate is outside of this range, and reduce the temperature of the animal heating system if the body temperature tends to exceed 37 °C.

1.10. Place the RF coil over the mouse.

NOTE: Depending on the system, this might require temporary disconnection of the ECG electrodes and respiratory balloon plugs from the ECG/respiratory interface module.

1.11. Connect the coil cables, and place the cradle in the magnet bore. Check if the ECG signal is still stable.

1.11.1. If the ECG signal is suboptimal, reposition the ECG electrodes for a better signal, as this cannot be done at a later stage without significantly changing the orientation of the animal.

[Place **Figure 1** here]

2. MRI scan calibration and triggering

2.1. Adjust the ECG and respiratory gating parameters within the ECG and respiratory signal monitoring software such that trigger points are generated at the R-peaks and only during the flat portion of the respiratory signal. To minimize ECG gating errors, set a blanking period that is 10–15 ms shorter than the R-R interval.

NOTE: This blanking period should be adjusted during the entire experiment if changes in heart rate occur.

2.2. Perform a center frequency calibration and a standard (ungated) SCOUT scan with zero offset to determine the position of the mouse in the scanner in coronal, axial, and sagittal directions. If the heart is not positioned within 0.5–1 cm of the field-of-view (FOV) center, adjust the position of the cradle accordingly, and redo the SCOUT scan.

2.3. Perform a manual shim and RF calibration using available vendor methods. See **Table 1** for detailed scan parameters of the following scans.

3. Scan planning and acquisition

3.1. Based on the initial SCOUT, perform a gated single-frame Gradient Echo (GRE) scout scan (**Table 1**, scan 1) with 5 slices in 3 orthogonal directions, and position each stack of slices on the approximate location of the heart to locate the exact position of the heart (**Figure 2A**).

3.2. Perform a gated single-frame multi-slice SA scout scan (**Table 1**, scan 2). To this end, use the previous GRE scout to position 4–5 slices in a mid-left ventricular position, perpendicular to the long axis of the heart to find an initial estimate of the short axis, which is needed to plan the long-axis 2-chamber scout (**Figure 2B**).

3.3. For the following prospective scans (steps 3.4–3.6), adjust the number of cardiac frames (Nframes) such that Nframes × TR is ~60–70% of the R-R interval.

NOTE: Acquisition for 60–70% of the R-R interval is enough to capture the end-diastolic phase of the cardiac cycle, while allowing additional T1 relaxation during end-diastole for improved SNR and preventing disturbance of the following R-peak by gradient switching.

3.4. Perform a gated single-slice GRE scan to generate the long-axis 2-chamber (2CH) scout, which combined with the SA scan, is needed to plan the 4-chamber (4CH) (**Table 1**, scan 3). To this end, position a slice perpendicular to the previous SA views running parallel to the connection points between the left and right ventricle. Move this slice to the middle of the left ventricle, and check in the coronal image of the GRE scout if the slice is aligned with the LV long axis such that it is placed through the apex (**Figure 2C**).

3.5. Perform another gated single-slice GRE scan to generate the 4-chamber (4CH) scout scan, which is needed to plan the multi-slice SA and the 3-chamber scan (**Table 1**, scan 4). To this end, position a slice perpendicular to the 2CH scout scan, and align to the center of the long axis such that the slice goes through the mitral valve and the apex. In the SA views, adjust the slice such that it is placed parallel to the posterior and anterior ventricular wall and between the two papillary muscles (**Figure 2D**). Check if the slice remains in the center of the ventricle throughout the entire cardiac cycle.

3.6. Perform a gated sequential multi-slice SA GRE scan (**Table 1**, scan 5) for systolic function measurements. To this end, position a midventricular slice perpendicular to the left ventricular long axis in the 2CH and 4CH views in the center of the heart, and increase the number of slices (typically an odd number, *e.g.,* 7 or 9 slices, no gap between the slices) to cover the heart from base to apex (**Figure 2E**).

3.7. For the following retrospectively gated scans (steps 3.8–3.9), turn off all prospective cardiac and respiratory gating functionality. Make note of the cardiac and respiratory rate before and after each retrospectively gated scan, and use these values for reconstruction purposes later (step 5.2.2).

3.8. Perform three sequential single-slice retrospectively gated GRE scans in short axis for quantification of the E’/A’ ratio, 2CH, and 4CH views, necessary for the quantification of the myocardial strain and HDF values (**Table 1**, scan 6-8). If needed, optimize the final 2CH and 4CH slice orientations based on the multi-slice short-axis views as well as the available 2CH and 4CH scout scans.

3.9. Perform an additional retrospectively gated single-slice GRE scan in a 3-chamber (3CH) view, which combined with the 2CH and 4CH view, is necessary for the quantification of the myocardial strain and HDF values (**Table 1**, scan 9). To this end, position a slice perpendicular on the midventricular short-axis view similar to the position of the final long-axis 4CH view, and turn the slice 45° to pass from the anterior wall to the papillary muscle closest to the posterior wall. Inspect the basal SA slice to see if the slice passes through the mitral and aortic valve. Inspect in the final long-axis 4CH view if the slice is going through the apex (**Figure 2F**).

[Place **Figure 2** here]
[Place **Table 1** here]

4. Finalization of the experiment and data storage

4.1. Remove the mouse from the cradle after detaching all other measurement equipment, and turn off the anesthesia. In the case of longitudinal experiments, place the mouse in a pre-warmed housing cage at 37 °C for recovery until the animal is awake and active.

4.2. Clean all equipment that has been used with cleaning wipes or 70% alcohol.

4.3. Generate Digital Imaging and Communication in Medicine (DICOM) files for the prospectively gated MRI data, and copy these together with the MRI raw data files of the retrospectively gated scans to a secure server for subsequent data analysis.

5 Offline reconstruction of the retrospectively acquired scans

NOTE: For the reconstruction of the retrospectively gated scans, a custom-built open-source software was used (**Figure 3**). Perform the following steps for each of the retrospectively triggered data separately.

5.1 Open the reconstruction software **Retrospective**, and load the raw data file corresponding to a retrospectively gated MRI scan.

5.2 Inspect the **Raw navigator** signal, and note that the higher signal peaks represent the respiratory frequency and the lower signal peaks represent the heart rate.

5.2.1 If the peaks are registered upside down, flip the signal with the **up/down** switch.

5.2.2 Additionally, check whether the automatically detected heart rate corresponds to 10% of the observed values during each scan. If not, manually adjust these values because automated detection failed.

5.2.3 Choose an appropriate window percentage for exclusion of data during respiratory movement, usually 30%.

5.3 Press **Filter** to perform the navigator analysis, and separate the heart navigator from the respiratory navigator.

5.4 Set the number of CINE frames to 32 (value used in this study), and press **sort k-space**.

5.5 Choose appropriate settings for compressed sensing (CS) regularization, and press **reconstruct**. Use the following typical regularization parameters: wavelet regularization parameter in the spatial (x, y, and z) dimensions (WVxyz) 0.001 or 0; total variation constraint in the CINE dimension (TVcine) 0.1; total variation constraint in spatial dimension (TVxyz) 0; and total variation constraint in the dynamics dimension (TVdyn) 0.05.

5.6 Once the reconstruction is finished, preview the CINE movie to evaluate the reconstruction. Export DICOM images for further analysis with **Export DCM**.

[Place **Figure 3** here]

6 Image analysis software

NOTE: The image analysis software (**Figure 4**) requires the use of DICOM images and has multiple plugins for different cardiovascular analysis applications, such as the plugin for volumetric measurements and the plugin for strain and HDF analysis.

6.1 For volumetric assessment of the LV, select the multi-slice SA scan, and load it into the plugin for volumetric measurements.

6.1.1 Assign end-systolic (ES) and end-diastolic (ED) labels to the corresponding cardiac frame.

6.1.2 Use the contour tools to segment the endomyocardial borders in the ES and ED frames.

NOTE: The analysis software, used for this protocol, automatically displays the LV EF, EDV, ESV parameters when all necessary annotations have been made.

6.2 For diastolic measurements, select the midventricular SA CINE images, and load these into the plugin for volumetric measurements.

6.2.1 Assign the ED and ES labels to the corresponding cardiac frames.

6.2.2 Use the contour tools to segment the endocardial border for all frames. Compare the segmentation of neighboring frames to ensure smooth transitions of the segmentation throughout the cardiac cycle.

6.2.3 Export the time evolution from all cardiac frames and corresponding LV endomyocardial volumes (LV ENDO). Apply a custom-built script (see **Supplemental Material**) to calculate the E'/A' ratio.

NOTE: The script applies a Savitzky-Golay filter for robust calculation of the dV/dt curves and uses semi-automatic peak detection to find the E' and A' peaks.

6.3 For strain and HDF calculations, select the 2CH, 3CH, and 4CH long-axis CINE images, and load them into the plugin for volumetric measurements.

6.3.1 Assign the ED and ES labels to the corresponding cardiac frame in each slice orientation.

6.3.2 Use the contour tools to segment the endocardial border for all frames in all 3 orientations. Compare the segmentation of neighboring frames to ensure smooth transitions of the segmentation throughout the cardiac cycle.

6.3.3 Once the contours are drawn in the plugin for volumetric measurements, run the plugin for the strain and HDF analysis.

6.3.4 Assign each of the acquired datasets to the corresponding labels for 2CH, 3CH, and 4CH views, and execute the strain analysis.

6.3.5 For HDF analysis, draw the diameter of the mitral valve at the end-diastolic frame in all 3 orientations, and draw the diameter of the aorta in the 3-chamber long-axis image.

[Place **Figure 4** here]

REPRESENTATIVE RESULTS:

Using the previously described protocol, a group of healthy C57BL/6 wildtype mice (n = 6, age 14 weeks) was scanned using a 7-Tesla MRI scanner using a 38-mm-diameter birdcage coil. During each scan session, the multi-slice CINE SA images were acquired using prospectively gated GRE sequences, while the single-slice midventricular SA, 2CH, 3CH, and 4CH views CINE images were acquired using retrospective gating. Representative high-frame rate reconstructions of retrospectively gated scans using a custom-built, post-processing software can be seen in **Supplemental Video 1**. From the resulting images, volume-time curves during the cardiac cycle (**Figure 5A**) were determined as well as the corresponding first-derivative curves (dV/dt) for calculation of systolic (EF = 72.4 ± 2.8%) and diastolic function parameters (E'/A' ratio = 1.5 ± 0.3) respectively.

The 2CH, 3CH, and 4CH view CINE images were analyzed using image analysis software to determine endocardial GLS (endoGLS) changes across the cardiac cycle (**Figure 5B**) and corresponding peak GLS values (-22.8 ± 2.4%) as a measure for myocardial strain. Additionally, the software calculates the root mean square (RMS) HDF in longitudinal (apex-base) (135.2 ± 31.7%) and transversal (inferolateral-anteroseptal) (12.9 ± 5.0%) directions. For each animal, it is also possible to produce an HDF time profile, which follows a consistent pattern of positive and negative peaks that represent the magnitude and direction of the HDF during the cardiac cycle (**Figure 5C**). Descriptive results of all outcome parameters are summarized in **Figure 5D**.

FIGURE AND TABLE LEGENDS:

Figure 1: Animal preparation and equipment setup for CMR imaging of the mouse heart. (**A**) Fully anesthetized mouse in the supine position, placed in the heated mouse cradle with a respiratory pneumatic pillow placed on the abdomen, rectal fiber-optic temperature sensor, and subcutaneous ECG leads in the chest near the forepaws. (**B**) Mouse body coil placed over the mouse cradle, with ECG leads and respiratory pillow reconnected to the ECG and respiratory interface prior to placing the holder in the MRI magnet. (**C**) Depiction of the ECG and respiratory signals in ECG and respiratory monitoring software. The R-peak of the ECG signal is detected and used as starting point for MRI signal acquisition. A blanking period between R-peaks can be manually adjusted based on the period of a heartbeat. Triggering can only occur during the respiratory plateau (green line in middle panel) for which the beginning delay and maximum width can be manually adjusted. Abbreviations: CMR = cardiovascular magnetic resonance imaging; ECG = electrocardiogram; MRI = magnetic resonance imaging.

Figure 2: Slice planning for CMR imaging in a mouse. (**A**) GRE SCOUT planning through the heart in 3 orthogonal views using initial scout scan. (**B**) Short-axis scout planning on the GRE SCOUT coronal and sagittal slices. (**C**) Planning of 2CH scout view using the short-axis scout and the GRE SCOUT coronal slice. (**D**) Planning of 4CH scout view using the short-axis scout and the 2CH scout. (**E**) Planning of the multi-slice short-axis view using 2CH and 4CH scouts. (**F**) (left) Planning of final 2CH, 3CH, and 4CH views using the midventricular short-axis and 2CH/4CH scout views. Abbreviations: CMR = cardiovascular magnetic resonance imaging; GRE = Gradient Echo; CH = chamber.

Figure 3: 'Retrospective' triggering graphical user interface. 'Retrospective' is a custom-built reconstruction application for retrospectively triggered cardiac magnetic resonance imaging scans. In the user interface, it is possible to evaluate the navigator signal, adjust the number of CINE frames to be reconstructed, adjust the compressed sensing parameters to improve reconstruction, preview the CINE images as a dynamic movie, and export the reconstructed data.

Figure 4: Image analysis software graphical user interface. The plugin for volumetric measurement in the image analysis software, which is used for contouring of the endomyocardial border. For each dataset, the end-diastolic and end-systolic cardiac phases are selected, and the endomyocardial border is segmented for all frames.

Figure 5: Quantification of LV functional parameters based on the mouse heart. (**A**) Representative volume-time curve and corresponding dV/dt curve. The latter depicts the flow velocity with distinct early filling peak (E') and atrial contraction (A') peaks. (**B**) Representative GLS curve indicating strain deformation in the longitudinal direction throughout the cardiac cycle. (**C**) Representative HDF curve with distinct force peaks in the apex-base direction, starting with the systolic ejection force and followed by a downward force at the transition between systole and diastole, E-wave deceleration force, A-wave acceleration, and deceleration force. (**D**) Descriptive results of all animals for values of EF, E'/A' ratio, peak GLS, and root mean square of the HDF in apex-base and inferolateral-anteroseptal directions. Values are expressed as mean ± SD. Abbreviations: LV = left ventricle; V = volume; t = time; GLS = global longitudinal strain; HDF = hemodynamic forces; EF = ejection fraction.

Table 1: Acquisition parameters for each sequence used during the CMR protocol. * Scans are performed in three different orthogonal orientations (axial, coronal, sagittal). **The shortest possible TE, given all other parameters are used, which depends on the specific scanner configuration. ***This is the number of cardiac frames after retrospective binning, **** The effective averaging depends on the random k-space filling during the total acquisition time. In total, 400 repetitions of all k-lines were performed. ***** Including ECG/respiratory triggering delays. Abbreviations: CMR = cardiovascular magnetic resonance imaging; ECG = electrocardiogram; GRE = gradient echo; FOV = field-of-view; TE = echo time; TR = repetition time; Nframes = number of cardiac frames; SA = short axis; CH = chamber.

Supplemental Video 1: Representative reconstruction of retrospectively gated CINE images in SA, 2CH, 3CH, and 4CH views. Abbreviations: SA = short axis; CH = chamber.

DISCUSSION:

The presented protocol describes the use of CMR imaging for longitudinal, non-invasive, *in vivo* experiments to analyze heart function in mice. These results are examples of healthy animals to demonstrate the feasibility of using CINE images to quantify the cardiac parameters. However, the methods described can be used for various animal models. Although specific disease models might require small alterations to the protocol, its basic structure to assess the different cardiac functional parameters will be the same. One particular case worth mentioning is a myocardial infarction model where part of the heart has significant loss in contractility. This can cause low quality of the cardiac navigator signal within this slice. In this case, an alternative option would be acquiring the navigator from a separate slice, as described in a previous study by Coolen et al.[16]. CINE images in different views are reconstructed from retrospectively gated data using CS algorithms and are analyzed using image analysis software to calculate the strain and HDF values.

The quality of the acquired images naturally depends on all preparation steps, which need to be carefully performed before starting the cardiac MRI protocol. For instance, if no clear ECG and respiratory signals are seen when placing the animal inside the MRI scanner, this will likely result in suboptimal acquisitions and even increased scan times due to the added effect of magnetohydrodynamic distortions[17]. It is important to realize that due to the sequential planning of the slice orientations, the animals cannot just be repositioned in between scans. It is therefore not possible to re-adjust the ECG leads in between scans, as this will alter the position of the mouse in the scanner. During scanning, temperature control is crucial for maintaining a constant cardiac and respiratory interval, which especially benefits the quality of the retrospectively gated scans that are acquired over a longer period of time. During this high-duty-cycle scan, the temperature of the animal might steadily increase, causing the heart rate and respiratory rate to increase. Adjusting the temperature of the heating system and the anesthesia could greatly contribute to stabilizing the respiratory rate prior to or during scanning.

A critical step during the analysis is the consistency in contour drawing. While automatic segmentation works well for clinical data, it does not perform robustly in the case of mouse cardiac data (not tested for rats). The high heart rate and high blood flow during specific cardiac phases, especially at the start of LV filling, may cause intravoxel dephasing and signal voids, compromising myocardial wall delineation. It is therefore not advised to analyze each frame independently, but visually inspect the motion of the myocardial wall between frames and take this into account when drawing the contours across all frames. It is advised to copy and adjust the endocardial contour between two consecutive frames to maintain a more natural contractile motion in the analysis. In this protocol, papillary muscles are excluded from the ventricular lumen volume in the SA images for systolic and diastolic function assessment, while they are included in the 2CH, 3CH, and 4CH views for strain and HDF analysis because the latter relies on knowledge of the precise motion of the myocardial wall, rather than the precise volume of the ventricular lumen.

Whereas systolic and diastolic function parameters are based on measuring LV volumes throughout the cardiac cycle, strain and HDF parameters depend on motion patterns within the myocardial wall as well. For this, feature-tracking techniques are used where the displacement of the myocardial segment can be assessed by recognizing distinct anatomical features and signal intensities between subsequent CINE phases. The strong contrast between blood pool and myocardium in CMR images facilitates the use of feature-tracking for subsequent strain and HDF analysis[8]. Prior to CMR feature-tracking, the myocardial strain was determined with speckle tracking echography and CMR tissue-tagging. CMR feature-tracking does not require additional scanning time compared to CMR tissue-tagging. However, despite the use of retrospective triggering, CMR still has a limited temporal resolution, which could make it difficult to correctly evaluate fast deformations within the cardiac cycle.

Assessment of HDF throughout the cardiac cycle requires measurements of the diameters of the mitral and aortic valves to calculate the HDF in apex-base and inferolateral-anteroseptal directions using previously described equations[18]. This method has shown consistent estimates of the HDF compared to the reference standard 4D-flow MRI, which has a limited availability in clinical use due to its complexity[6]. It is important to know that robust estimation of the valve diameters is difficult, and therefore, the valve diameters should be kept constant for a group of animals and across repeated measurements in a longitudinal study, as variations in this parameter by incorrect estimations could easily overshadow subtle changes in HDF parameters. The specific software used to calculate GLS and HDF parameters might not be available to all users. Therefore, one can refer to Voigt et al.[19] (GLS) as well as Pedrizzetti et al.[6,20] (HDF), which contain all mathematical descriptions that form the basis of the respective calculations as performed by the analysis software.

For the purpose of this study, the protocol was evaluated in healthy animals (N = 6). A representative set of time curves for LV volume, dV/dt, endoGLS, and HDF are shown in **Figure 5A–C**. Mean values of multiple cardiac functional parameters (EF, E'/A'-ratio, peak GLS, and HDF) are shown in **Figure 5D**. These agree well with comparable protocols used in the literature[21]. Literature on GLS and HDF data in mice is scarce. A mean GLS value of -22.8% was measured, which is in the same range as clinical data[8], indicating that GLS measurements obtained with the described method are feasible in mice. HDF curves obtained in mice also show the same distinct phases as seen in human data, showing the successful translation of this technique to preclinical research. While HDF parameters are hypothesized to serve as early biomarkers of cardiac dysfunction, more studies are warranted to investigate the diagnostic and predictive value of this new parameter. The results in this protocol do show that HDF and GLS outcomes are expected to be more variable across animals, which needs to be taken into account when subtle differences in animal models or treatment effects are expected.

ACKNOWLEDGMENTS:

The authors thank Dorita Dekkers and Fatimah Al Darwish for assistance with the mouse measurements and data analysis.

DISCLOSURES:

Ruslan Garipov is an employee of MR Solutions Ltd., Guildford, United Kingdom. David Hautemann is an employee of Medis medical imaging systems B.V., Leiden, The Netherlands.

REFERENCES:

1. Vallée, J. P., Ivancevic, M. K., Nguyen, D., Morel, D. R. , Jaconi, M. Current status of cardiac MRI in small animals. *Magnetic Resononance Materials in Physics, Biology and Medicine.* **17** (3–6), 149–156 (2004).
2. Bakermans, A. J. et al. Small animal cardiovascular MR imaging and spectroscopy. *Progress in Nuclear Magnetic Resonance Spectroscopy.* **88**–**89**, 1–47 (2015).
3. Wu, Y. L. , Lo, C. W. Diverse application of MRI for mouse phenotyping. *Birth Defects Research.* **109** (10), 758–770 (2017).
4. Coolen, B. F. et al. High frame rate retrospectively triggered Cine MRI for assessment of murine diastolic function. *Magnetic Resonance in Medicine.* **69** (3), 648–656 (2013).
5. Lapinskas, T. et al. Cardiovascular magnetic resonance feature tracking in small animals - a preliminary study on reproducibility and sample size calculation. *BMC Medical Imaging.* **17** (1), 51 (2017).
6. Pedrizzetti, G. et al. On estimating intraventricular hemodynamic forces from endocardial dynamics: A comparative study with 4D flow MRI. *Journal of Biomechanics.* **60**, 203–210 (2017).
7. Motaal, A. G. et al. Accelerated high-frame-rate mouse heart cine-MRI using compressed sensing reconstruction. *NMR in Biomedicine.* **26** (4), 451–457 (2013).
8. Claus, P., Omar, A. M. S., Pedrizzetti, G., Sengupta, P. P., Nagel, E. Tissue tracking technology for assessing cardiac mechanics: principles, normal values, and clinical applications. *JACC. Cardiovascular Imaging.* **8** (12), 1444–1460 (2015).
9. Scatteia, A., Baritussio, A., Bucciarelli-Ducci, C. Strain imaging using cardiac magnetic resonance. *Heart Failure Reviews.* **22** (4), 465–476 (2017).
10. Modin, D., Andersen, D. M., Biering-Sørensen, T. Echo and heart failure: when do people need an echo, and when do they need natriuretic peptides? *Echo Research and Practice.* **5** (2), R65–R79 (2018).
11. Onishi, T. et al. Longitudinal strain and global circumferential strain by speckle-tracking echocardiography and feature-tracking cardiac magnetic resonance imaging: comparison with left ventricular ejection fraction. *Journal of American Society of Echocardiography.* **28** (5), 587–596 (2015).
12. Faganello, G. et al. A new integrated approach to cardiac mechanics: reference values for normal left ventricle. *The International Journal of Cardiovascular Imaging.* **36,** 2173-2185 (2020).
13. Lapinskas, T. et al. The intraventricular hemodynamic forces estimated using routine CMR Cine images: a new marker of the failing heart. *JACC. Cardiovascular Imaging.* **12** (2), 377–379 (2019).
14. Töger, J. et al. Intracardiac hemodynamic forces using 4D flow: a new reproducible method applied to healthy controls, elite athletes and heart failure patients. *Journal of Cardiovascular Magnetic Resonance.* **18** (Suppl 1), Q61 (2016).
15. Eriksson, J., Bolger, A. F., Ebbers, T., Carlhäll, C. J. Assessment of left ventricular hemodynamic forces in healthy subjects and patients with dilated cardiomyopathy using 4D flow MRI. *Physiological Reports.* **4** (3), e12685 (2016).
16. Coolen, B. F. et al. Three-dimensional T1 mapping of the mouse heart using variable flip angle steady-state MR imaging. *NMR in Biomedicine.* **24** (2), 154–162 (2011).
17. Nijm, G. M., Swiryn, S., Larson, A. C., Sahakian, A. V. Characterization of the

magnetohydrodynamic effect as a signal from the surface electrocardiogram during cardiac magnetic resonance imaging. *Computers in Cardiology.* **33**, 269–272 (2006).

18. Domenichini, F., Pedrizzetti, G. Hemodynamic forces in a model left ventricle. *Physical Review Fluids.* **1**, 083201 (2016).

19. Voigt, J. U. et al. Definitions for a common standard for 2D speckle tracking echocardiography: consensus document of the EACVI/ASE/Industry Task Force to standardize deformation imaging. *European Heart Journal - Cardiovascular Imaging.* **16** (1), 1–11 (2015).

20. Pedrizzetti, G. On the computation of hemodynamic forces in the heart chambers. *Journal of Biomechanics.* **95**, 109323 (2019).

21. Hoffman, M. et al. Myocardial strain and cardiac output are preferable measurements for cardiac dysfunction and can predict mortality in septic mice. *Journal of American Heart Association.* **8** (10), e012260 (2019).

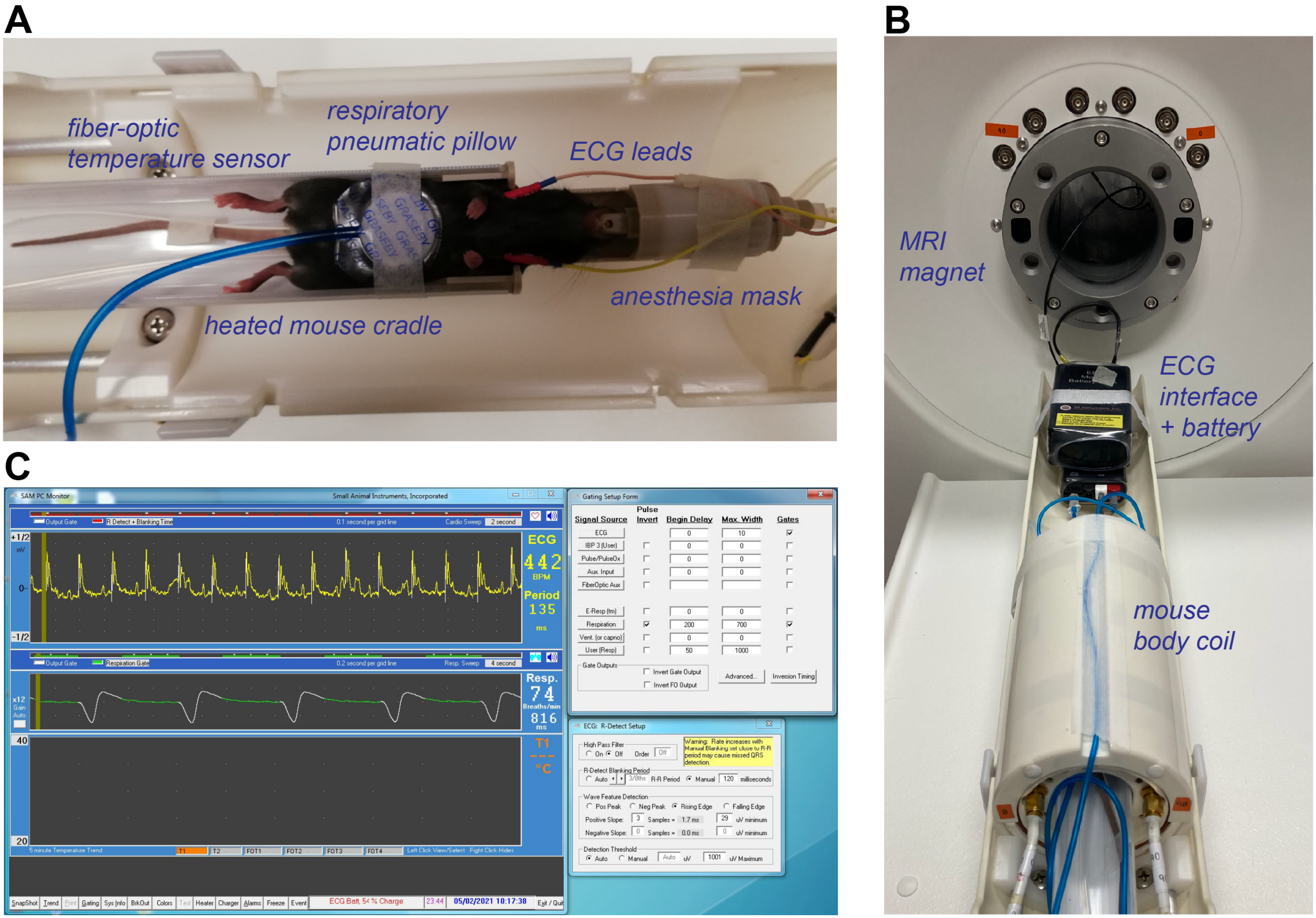

Gating Setup Form

Signal Source	Pulse Invert	Begin Delay	Max. Width	Gates
ECG		0	10	☑
IBP 3 (User)	☐	0	0	☐
Pulse/PulseOx	☐	0	0	☐
Aux. Input	☐	0	0	☐
FiberOptic Aux	☐			☐
E-Resp (tm)	☐	0	0	☐
Respiration	☑	200	700	☑
Vent. (or capno)	☐	0	0	☐
User (Resp)	☐	50	1000	☐

Gate Outputs
☐ Invert Gate Output
☐ Invert FO Output

ECG: R-Detect Setup

High Pass Filter
○ On ● Off Order Off

Warning: Rate increases with Manual Blanking set close to R-R period may cause missed QRS detection.

R-Detect Blanking Period
○ Auto 3/8ths R-R Period ● Manual 120 milliseconds

Wave Feature Detection
○ Pos Peak ○ Neg Peak ● Rising Edge ○ Falling Edge
Positive Slope: 3 Samples = 1.7 ms 29 uV minimum
Negative Slope: 0 Samples = 0.0 ms 0 uV minimum

Detection Threshold
● Auto ○ Manual Auto uV 1001 uV Maximum

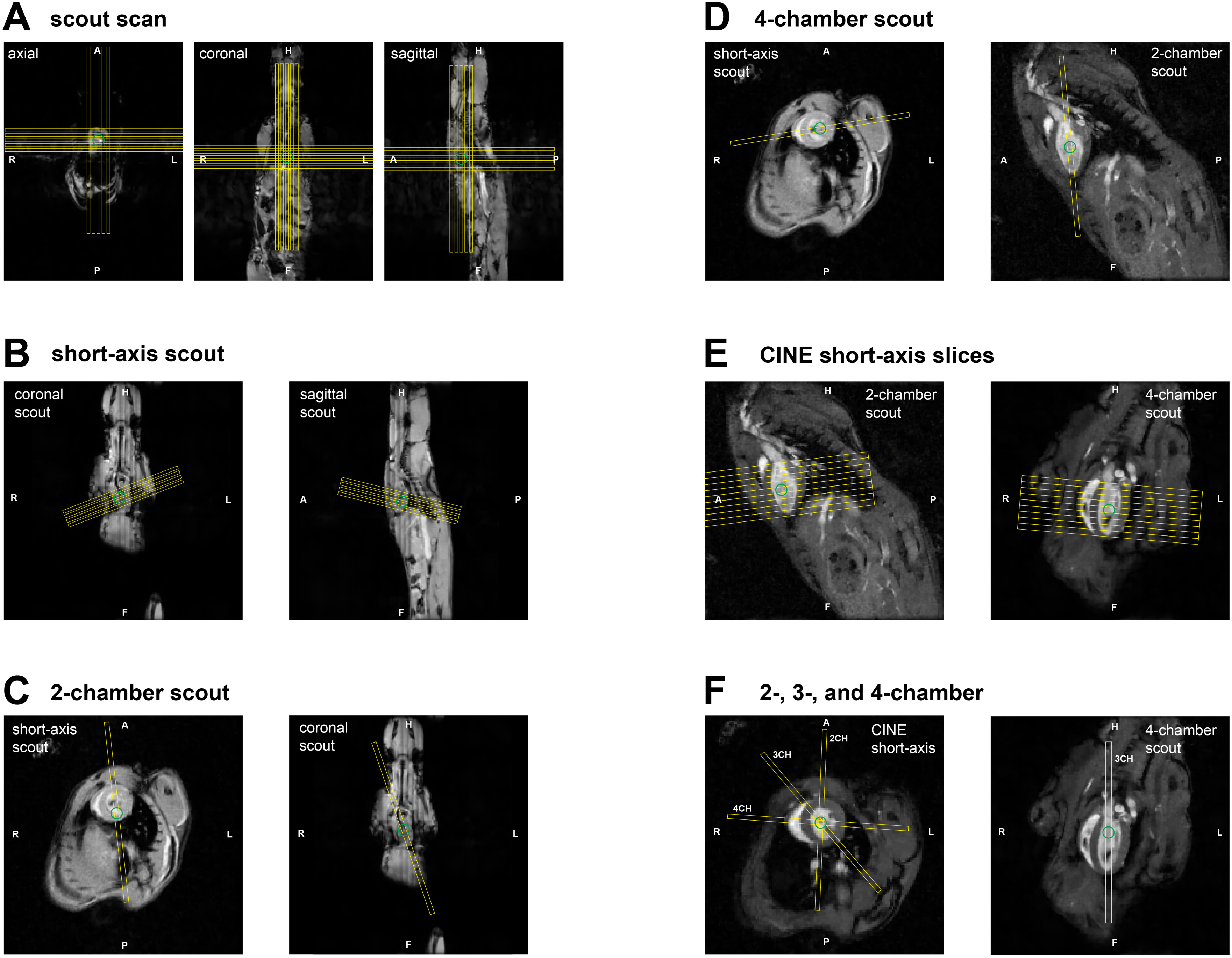
A scout scan
axial
coronal
sagittal
A
P
R
L
H
F
B short-axis scout
coronal scout
sagittal scout
C 2-chamber scout
short-axis scout
coronal scout
D 4-chamber scout
short-axis scout
2-chamber scout
E CINE short-axis slices
2-chamber scout
4-chamber scout
F 2-, 3-, and 4-chamber
CINE short-axis
2CH
3CH
4CH
4-chamber scout
3CH

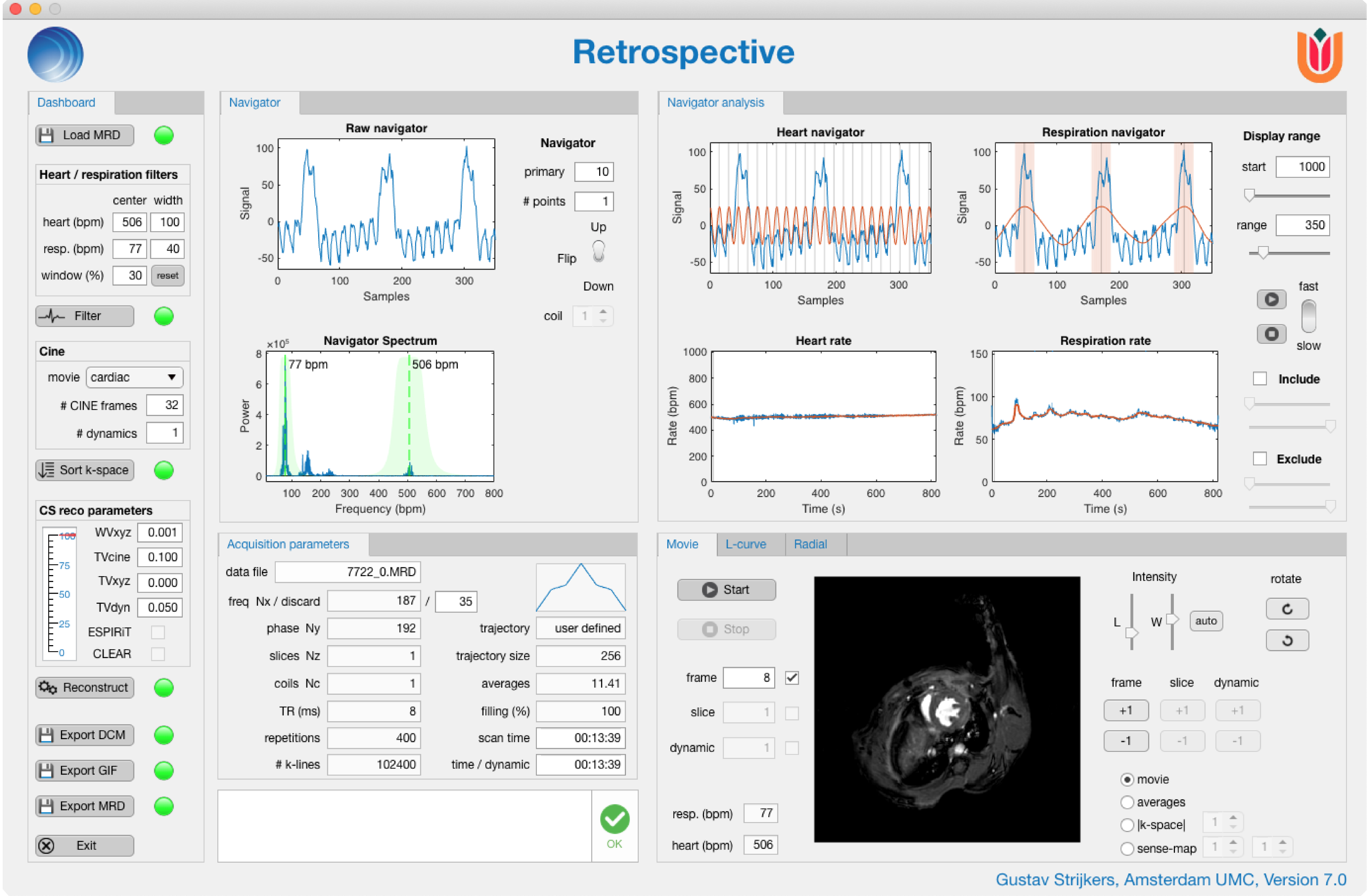

heart (bpm) center 506 width 100

resp. (bpm) center 77 width 40

window (%) 30

movie cardiac

CINE frames 32

dynamics 1

WVxyz 0.001

TVcine 0.100

TVxyz 0.000

TVdyn 0.050

ESPIRiT ☐

CLEAR ☐

Navigator

primary 10

points 1

coil 1

start 1000

range 350

☐ Include

☐ Exclude

data file 7722_0.MRD

freq Nx / discard 187 / 35

phase Ny 192

slices Nz 1

coils Nc 1

TR (ms) 8

repetitions 400

k-lines 102400

trajectory user defined

trajectory size 256

averages 11.41

filling (%) 100

scan time 00:13:39

time / dynamic 00:13:39

frame 8 ☑

slice 1 ☐

dynamic 1 ☐

resp. (bpm) 77

heart (bpm) 506

frame slice dynamic

● movie

○ averages

○ |k-space| 1

○ sense-map 1 1

Gustav Strijkers, Amsterdam UMC, Version 7.0

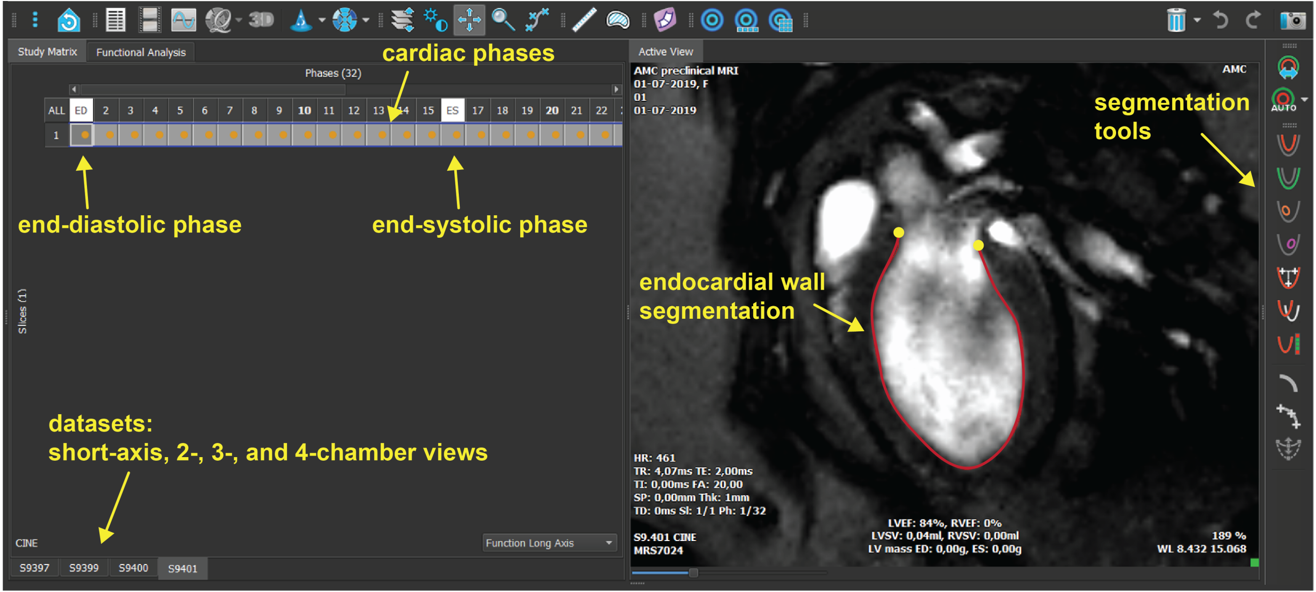
cardiac phases

end-diastolic phase

end-systolic phase

datasets:
short-axis, 2-, 3-, and 4-chamber views

endocardial wall segmentation

segmentation tools

AMC preclinical MRI
01-07-2019, F
01
01-07-2019

HR: 461
TR: 4,07ms TE: 2,00ms
TI: 0,00ms FA: 20,00
SP: 0,00mm Thk: 1mm
TD: 0ms Sl: 1/1 Ph: 1/32

S9.401 CINE
MRS7024

LVEF: 84%, RVEF: 0%
LVSV: 0,04ml, RVSV: 0,00ml
LV mass ED: 0,00g, ES: 0,00g

189 %
WL 8.432 15.068

Figure 5

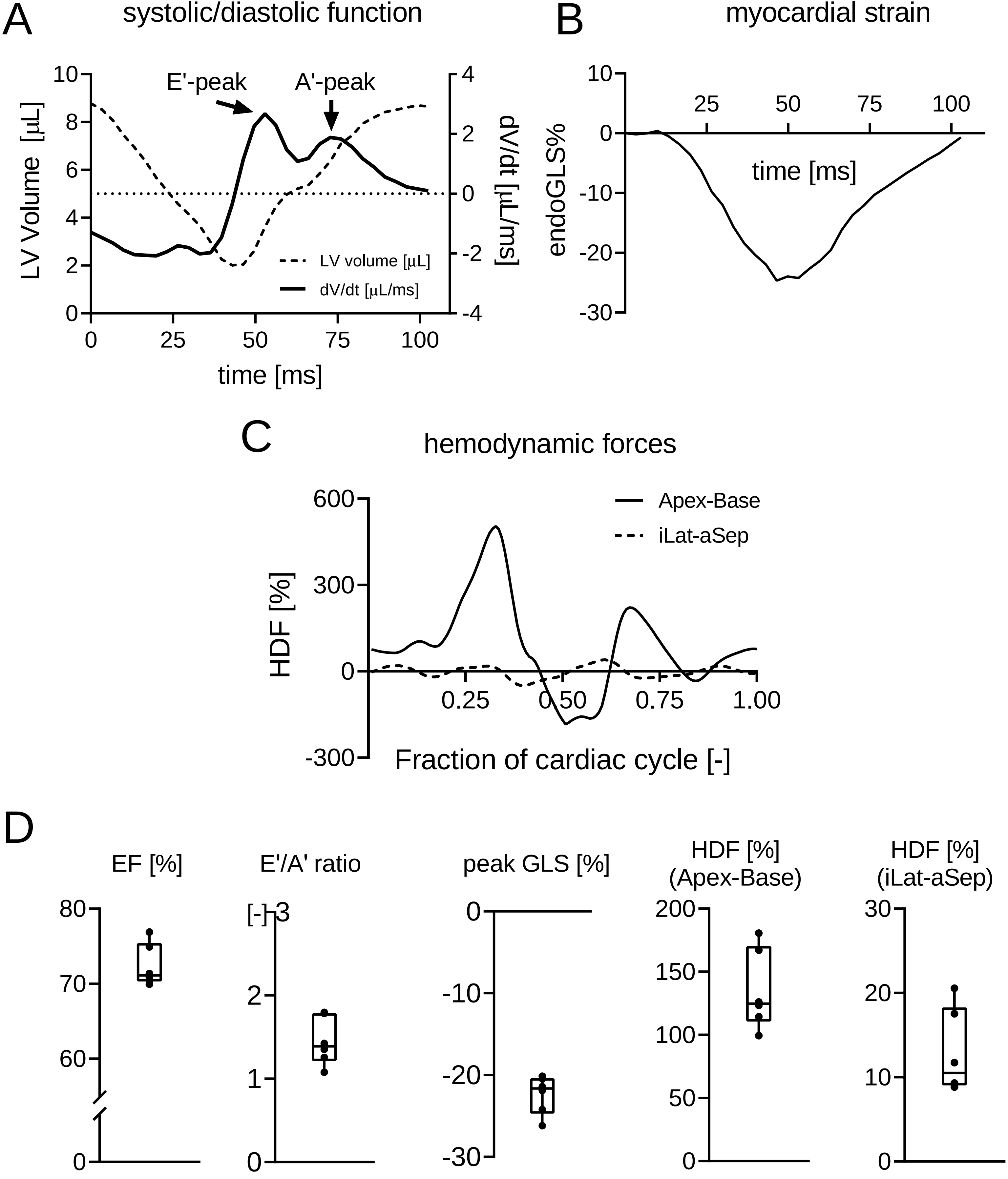
A
systolic/diastolic function
E'-peak
A'-peak
LV Volume [µL]
dV/dt [µL/ms]
LV volume [µL]
dV/dt [µL/ms]
10
8
6
4
2
0
4
2
0
-2
-4
0
25
50
75
100
time [ms]
B
myocardial strain
endoGLS%
10
0
-10
-20
-30
25
50
75
100
time [ms]
C
hemodynamic forces
HDF [%]
Apex-Base
iLat-aSep
600
300
0
-300
0.25
0.50
0.75
1.00
Fraction of cardiac cycle [-]
D
EF [%]
80
70
60
0
E'/A' ratio
[-] 3
2
1
0
peak GLS [%]
0
-10
-20
-30
HDF [%] (Apex-Base)
200
150
100
50
0
HDF [%] (iLat-aSep)
30
20
10
0

Table 1.Acquisition parameters for each sequence used during the CMR protocol.

Scan number(s)	1	2
Scan name(s)	GRE scout	multi-slice SA scout
total slices	15 (3 x 5)*	4-5
Thickness (mm)	1	1
FOV (mm)	60	35
FOV Ratio	1	1
Flip Angle	40	20
TE (ms)**	3.8	3.4
TR (ms)	200	1 R-R
Nframes	1	1
Matrix Size	192 x 192	192 x 192
ECG triggering	no	yes
Respiratory triggering	yes	yes
Averages	1	3
Total imaging time (estimated ***)**	2 min	2min

3	4	5	6-9
2CH scout	4CH scout	multi-slice SA	SA, 2CH, 4CH, 3CH
1	1	7-9	1
1	1	1	1
30	30	35	30
1	1	1	1
20	20	20	15
2.5	2.5	2.5	3.6
7	7	7	8
12-14	12-14	12-14	32 ***
192 x 192	192 x 192	192 x 192	192 x 192
yes	yes	yes	retrospective
yes	yes	yes	retrospective
5	5	5	retrospective ****
3-4 min	3-4 min	20-25 min	13 min / scan

Name of Material/ Equipment	Company	Catalog Number
Equipment		
AccuSens single and multi-channel signal conditioner	Opsens solutions inc., Canada	ACS-P4-N-62SC
Duratears eye ointment	Alcon Nederland B.V., Netherlands	
Mouse cell	Équipment Vétérinaire Minerve, France	
MR-compatible Monitoring & Gating System for Small animals	SA Intuments, Inc., United States	Model 1030
MRI scanner	MR Solutions Ltd., United Kingdom	Model: MRS-7024
Multistation temperature control unit and High Flow PCA	Équipment Vétérinaire Minerve, France	Model: URT Multipostes
Respiration Sensor	Graseby Medical Limited, United Kingdom	Ref 2005100
RF coil	MR Solutions Ltd., United Kingdom	MRS-MVC
SF flowmeter	flow-meter, Italy	SF 3
Vaporizer sigma delta Intermed	Penlon Ltd., United Kingdom	
Materials		
Isoflurane	AST farma, Netherlands	
Vaseline petroleum jelly	Unilever, United Kingdom	
Software		
BART toolbox		
Mathematica 12.0	Wolfram Research, Inc., United States	
MATLAB 2019a	The MathWorks,Inc., United States	
MEDIS Suite MR	Medis Medical Imaging Systems B.V. ,Netherlands	
PC-SAM	SA Intuments, Inc., United States	
Preclinical Scan	MR Solutions Ltd., United Kingdom	
Retrospective version 7.0	Amsterdam UMC, the Netherlands	

Comments/Description
Used with fiber optic temperature sensor to monitor body temperature
referred to as mouse cradle
ERT Module (ECG/respiratory interface module) , ERT Control/Gating Module, battery pack and subdermal ECG Electrode Set
Preclinical MRI System 7.0T/24 cm
animal heating system
38mm mouse volume RF coil for mouse body studies
https://mrirecon.github.io/bart/
Image analysis software
Scanning software
Reconstuction software: https://github.com/Moby1971?tab=repositories

Editorial comments

E1

Please take this opportunity to thoroughly proofread the manuscript to ensure that there are no spelling or grammar issues.

Grammar and spelling errors have been corrected to the best of our abilities.

E2

Please revise the text to avoid the use of any personal pronouns (e.g., "we", "you", "our" etc.).

Personal pronouns have been removed.

E3

JoVE cannot publish manuscripts containing commercial language. This includes trademark symbols (™), registered symbols (®), and company names before an instrument or reagent. Please remove all commercial language from your manuscript and use generic terms instead. All commercial products should be sufficiently referenced in the Table of Materials.
For example: MEDIS Suite image analysis software, Mathematica 12.0, PC-SAM, etc.

Commercial software names have been removed from the protocol. The only software name in the protocol is that of our own application. The company names of the software used, are still cited in the Table of Materials.

E4

Please ensure that all text in the protocol section is written in the imperative tense as if telling someone how to do the technique (e.g., “Do this,” “Ensure that,” etc.). The actions should be described in the imperative tense in complete sentences wherever possible. Avoid usage of phrases such as “could be,” “should be,” and “would be” throughout the Protocol. Any text that cannot be written in the imperative tense may be added as a “Note.” However, notes should be concise and used sparingly. Please include all safety procedures and use of hoods, etc.

Where possible, the sentence is changed to imperative tense. For text where this was not possible, the information is added as a note as they did not fit in the discussion.

The text has been revised with the following sentence to indicate the necessity of a fume removal tube in the scanner area to remove excess isoflurane.

“Make sure the scanner area is equipped with a working fume extraction tube to remove excess isoflurane.”

The text has been revised with the following sentence to indicate the use of a fume hood extraction arm during the induction of the animal.

“Place the mouse in an anesthesia induction chamber under a fume hood extraction arm and provide 3-4 % isoflurane in a mixture of 0.2 L/min O_2 and 0.2 L/min medical air.”

E5

The Protocol should contain only action items that direct the reader to do something. Please move the discussion about the protocol to the Discussion.

The protocol has been revised to only contain only action items and notes that cannot be written in the imperative tense. These notes contain small points the reader must keep in mind while executing this protocol. We did not move these notes to the discussion, as doing so would drastically alter the structure of the discussion. Any remaining discussion about the protocol has been moved to the discussion section of the manuscript.

E6

Please include a one-line space between each protocol step and then highlight up to 3 pages of the Protocol (including headings and spacing) that identifies the essential steps of the protocol for the video, i.e., the steps that should be visualized to tell the most cohesive story of the Protocol. Remember that non-highlighted Protocol steps will remain in the manuscript, and therefore will still be available to the reader.

A one-line space has been added between each protocol step, sub-step, and notes. The highlighted steps are together no more than 3 pages.

E7

When giving a reference in the text, ensure that the corresponding number from the reference list appears superscripted without a space after the word/group of words it applies to but before any punctuation (in the case of et al., place the superscripted number after et al. but before other punctuation).

All reference numbers are now before punctuation.

E8

Please do not use the &-sign or the word “and” when listing authors in the reference section. Title case and italicize journal titles and book titles. Do not use any abbreviations. Article titles should start with a capital letter and end with a period and should appear exactly as they were published in the original work, without any abbreviations or truncations.

Titles have been edited to appear exactly as they were published, abbreviations in titles only remained if that is how they appeared in the original work. The & -symbol as well as ‘and’ have been removed from the list of authors. Journal names are written out without abbreviations and are italicized.

E9

Figure 5: Please revise the y-axis unit of figure 5A to “µL” instead of “µl”.

The y-axis unit, as well as the legend of figure 5A, are revised.

Reviewer #1

Manuscript Summary:
This manuscript describes a routine full left ventricular morphology/function assessment in mice using MRI at 7 tesla.
It highlights the important steps to conduct a protocol, gives standard parameters for MRI sequences and hints for an optimal and reproducible workflow. I should highlight that the authors present and share their code for an optimized retrospective reconstruction tool.
The manuscript is well organized and in good language. Illustrations are very helpful to those planning to do such exams. I have only two small additions to suggest.

We thank the reviewer for his/her positive remarks concerning our manuscript, but also for raising some important concerns, which are addressed below.

R1.1

The LV segmentation / evaluation is done using a specific proprietary software (MASS), and there is no mention of other options, so there is some promotional aspect that may not be desirable in this journal. Would it be possible to point that out in on sentence ahead of the description and to give links to other tools available?

The brand names of the software we used have been removed from the manuscript to avoid the promotional aspect.

R1.2

The parameter list may be too restrictive (or vice versa too relaxed) for certain scanner models in terms of TE, TR, FOV, RF coil available, etc. At least for TE the authors may find useful to point out that it should be set to the minimum achievable (flow artifacts).

The description of the parameter list is revised to indicate that the values are applicable to our system. In particular, it is advised to use the shortest possible TE of your system.

“**The shortest possible TE given all other parameters should be used, which depends on the specific scanner configuration.”

Reviewer #2

The present manuscript by Daal et al. describes in detail how to carry out quantification of left ventricular function, myocardial strain, and hemodynamic forces of the mouse heart by cardiovascular magnetic resonance imaging (MRI). The paper is overall clearly written and a valid contribution by a group with long-standing experience in cardiovascular MRI of mice. The described protocol will be very useful for users unexperienced in cardiac MRI. I have a few comments, how this work could further be improved.

We thank the reviewer for carefully reviewing our paper and providing us feedback to further improve our manuscript.

R2.1

1. Point 1.2: Turn on the animal heating system with the temperature set to 40 °C. This seems to me a bit hot. Body temperature of mice is around 38 °C. Please comment.

The internal temperature of the animal should always be monitored and the heating system adjusted accordingly. In our experience, the body temperature of the mouse is always somewhat lower than that of the heating system. Therefore, setting the heating system to 40 °C helps maintain a normal body temperature of the mouse of around 36-37°C during and after preparation. Throughout the scan session, it is possible that the body temperature slowly starts to increase. At this point, you should indeed decrease the temperature of the heating system to prevent the body temperature from exceeding 37 °C.

With the following sentence, we have indicated in the manuscript that the temperature of the heating system needs to be lowered from the initial value if the body temperature exceeds 37°C.

"Adjust the isoflurane administration when the respiratory rate is outside of this range and reduce the temperature of the animal heating system if the body temperature tends to exceed 37 °C."

R2.2

Point 1.5: What's about an active isoflurane removal system? Over time this accumulates in the laboratory and long-term exposure may cause chronic or adverse health effects including nausea, dizziness, fatigue etc.

At the back opening of the scanner, there is an air extraction tube for the removal of excess isoflurane in the scanner bore. Although this is a specific setup in our lab and might differ from other labs. The text has been revised with the following sentence to indicate the necessity of a fume removal tube in the scanner area to remove excess isoflurane.

"Make sure the scanner area is equipped with a working fume extraction tube to remove excess isoflurane."

The induction chamber is under a benchtop fume extraction arm for the removal of isoflurane. The text has been revised with the following sentence to indicate the use of a fume hood extraction arm during the induction of the animal.

"Place the mouse in an anesthesia induction chamber under a fume hood extraction arm and provide 3-4 % isoflurane in a mixture of 0.2 L/min O_2 and 0.2 L/min medical air."

R2.3

Figure 1c: It seems that the width of the respiratory gate has been chosen a bit too long with detection of a QRS complex already in inspiration (at least for the last respiratory cycles shown in the screen shot). This will result in motion artefacts which affect image quality. Here or elsewhere, you may also mention that in particular in the case of bad ECG quality (e.g. after myocardial infarction) the wave feature detection of rising/falling edge is always superior over positive/negative peak.

We agree with the reviewer that our representative example of ECG/respiratory gating signals was suboptimal and that the respiratory gating interval should have been slightly shortened in order to prevent acquisition during inspiration. We now adapted this in our representative example to prevent confusion with the reader.

R2.4

Points 3.1-3.9: During the protocol explain a bit more in detail, which scan is required for which purpose.

We have provided more detailed explanations of which scan is used for which purpose. From the revised protocol, it is important that the reader understands which scans are needed to plan the orientation of the scans that will eventually be used for analysis, which in this case the multi-slice short-axis scan and the retrospectively triggered scans in SA, 2CH, 3CH, and 4CH view.

The following sentences have been revised to reflect this.

"Based on the initial SCOUT, perform a gated single-frame Gradient Echo (GRE) scout scan (Table 1, scan 1) with 5 slices in 3 orthogonal directions and position each stack of slices on the approximate location of the heart in order to locate the exact position of the heart (Figure 2A)."

"To this end, use the previous GRE scout to position 4-5 slices in a mid-left ventricular position perpendicular on the long axis of the heart in order to find an initial estimate of the short axis which is needed to plan the long-axis 2-chamber scout (Figure 2B)."

"Perform a gated single-slice GRE scan to generate the long-axis 2-chamber (2CH) scout which combined with the short-axis scan, is needed to plan the 4-chamber (4CH) (Table 1, scan 3)."

"Perform another gated single-slice GRE scan to generate the 4-chamber (4CH) scout scan which is needed to plan the multi-slice SA and the 3-chamber scan (Table 1, scan 4)."

"Perform three sequential single-slice retrospectively gated GRE scans in respectively short-axis for quantification of the E'/A' ratio, 2CH, and 4CH views, necessary for the quantification of the myocardial strain and HDF values (Table 1, scan 6-8)."

"Perform an additional retrospectively gated single-slice GRE scan in a 3-chamber (3CH) view which combined with the 2CH and 4CH view is necessary for the quantification of the myocardial strain and HDF values (Table 1, scan 9)."

R2.5

Can you explain, why you use a prospectively gated CINE sequence for systolic function measurements but for all other analysis retrospectively gated sequences?

Although it would indeed be possible to perform the retrospectively gated sequence for systolic function, we chose to perform prospective gating for two reasons: 1) many users still perform ECG gated sequences and we therefore wanted to include both strategies (prospective and retrospective)

Secondly, retrospective triggering, while being a powerful tool to achieve high temporal resolution CINES needed for GLS and HDF analysis, is less time efficient than prospective gating, especially when end-diastolic information is not needed as is the case for EF measurements. Therefore, prospective triggering is very well suited for fast planning of cardiac orientations as well as performing the multi-slice systolic function measurements.

R2.6

When I got you right you are doing the reconstruction with your own tools and afterwards you export the data for analysis with the MEDIS Suite. Maybe, you should state a bit more clearly that you require the DICOM export for assessing the data by MEDIS.

The text has been revised with the following sentence to indicate the use of DICOM images in the analysis software.

"The image analysis software (Figure 4) requires the use of DICOM images and has multiple plugins for different cardiovascular analysis applications, such as the plugin for volumetric measurements and the plugin for strain and HDF analysis."

R2.7

You are using MEDIS for a semi-automatic analysis of all parameters. However, this is somehow a black-box approach and, furthermore, a quite expensive proprietary software. I feel you should include also the relevant equations for calculation of GLS, HDF etc. at least into the appendix/supplement, so that each user can use its own solution for data evaluation.

We are aware that especially the HDF analysis is quite complex, however, we strongly feel it is beyond the scope of this manuscript to repeat the physics behind the algorithms used in the MEDIS software to calculate HDF. Instead, we prefer to refer to the appropriate literature, which forms the basis of the calculations used in the MEDIS software. Specifically, we added the following section:

"The specific software used to calculate GLS and HDF parameters might not be available to all users. Therefore, one can refer to Voigt et al.[19] (GLS) as well as Pedrizzetti et al.[6,20](HDF), which contain all mathematical descriptions that form the basis of the respective calculations as performed by the analysis software."

[Voigt *et al. European Heart Journal - Cardiovascular Imaging* 2015;16:1-11].
[Pedrizzetti *et al. Journal of Biomechanics* 2017;60:203-210].
[Pedrizzetti. *Journal of Biomechanics* 2019; 95: 109323].

R2.8

I suggest to include also some sample data from a disease model, such as myocardial infarction or hypertrophy models, so that the reader can get a feeling which functional alterations can be expected.

While we respect the comment of the reviewer, we deliberately chose to do experiments in healthy animals as this provides a good reference to perform the different measurements of our protocol as well as the subsequent analyses. However, because we agree it's important to indicate the use of our protocol in disease models, we added the following sentences to the Discussion:

"The presented results are examples of healthy animals, in order to demonstrate the feasibility of using CINE images to quantify the cardiac parameters. However, the methods described can be used for various animal models. Although specific disease models might require small alterations to the protocol, its basic structure to assess the different cardiac functional parameters will be the same. One particular case worth mentioning is a myocardial infarction model where part of the heart has

significant loss in contractility. This can cause low quality of the cardiac navigator signal within this slice. In this case, an alternative option would be acquiring the navigator from a separate slice, as described in a previous study by Coolen et al .[16]*"*

[Coolen *et al*. *NMR in Biomedicine* 2011; 24: 154-162].

R2.9

Discussion: Inclusion/exclusion of the papillary muscle - this is a bit confusing. From what to you include/exclude them?

We agree this was not clearly written. What is meant is that the papillary muscles are included or excluded from the ventricular lumen volume.

The text has been revised to the following to make this more clear.

"In this protocol, papillary muscles are excluded from the ventricular lumen volume in the short-axis images for systolic and diastolic function assessment, while they are included in the 2CH, 3CH, and 4CH views for strain and HDF analysis because the latter relies on knowledge of the precise motion of the myocardial wall, rather than the precise volume of the ventricular lumen."

R2.10

Discussion: 'We therefore advise to keep valve diameters constant for a group of animals and across different time points'. This is also confusing, how can I keep valve diameters constant, when their alterations over the cardiac cycle are used to calculate HDF? Please clarify.

We understand the confusion with the reviewer. The time points, in this case, are repeated measurements in case a longitudinal study is performed.

The text has been revised to clarify this as follows.

"It is important to know that robust estimation of the valve diameters is difficult and therefore, the valve diameter should be kept constant for a group of animals and across repeated measurements in a longitudinal study as variations in this parameter by incorrect estimations could easily overshadow subtle changes in HDF parameters."

Reviewer #3:

Manuscript Summary:

Manuscript "Quantification of left ventricular function, myocardial strain, and hemodynamic forces of the mouse heart by cardiovascular magnetic resonance imaging" describes magnetic resonance imaging technique to perform preparations, measurements and data analysis for cardiac strain analysis. Mouse cardiac models are widely used, and provide a good and cost effective living model to study human cardiac pathologies. MRI provides accurate cardiac functional measures containing strain and hemodynamic forces among more traditional ejection fraction, cardiac output and myocardial mass. Based on these facts, the methodology described in this manuscript has potential to be used in several laboratories and it provides a good starting point for researchers to begin with mouse cardiac imaging.

We thank the reviewer for his/her appreciation of our manuscript with no further comments to address.

Supplemental Movie 1.Representative reconstruction of retrospectively gated CINE images in SA, 2CH, 3CH, and 4CH

Click here to access/download

Supplemental Coding Files

Supplemental_Material_movie.mp4

Mathematica script